IEEE Access
Multidisciplinary | Rapid Review | Open Access Journal

Received April 9, 2021, accepted April 22, 2021, date of publication April 29, 2021, date of current version May 5, 2021.

Digital Object Identifier 10.1109/ACCESS.2021.3076493

Bandwidth-Enhanced Low-Profile Magneto-Electric Dipole Antenna With Shorting Parasitic Elements

SON TRINH-VAN, THAI VAN TRINH, YOUNGOO YANG, (Senior Member, IEEE), KANG-YOON LEE, (Senior Member, IEEE), AND KEUM CHEOL HWANG, (Senior Member, IEEE)

Department of Electrical and Computer Engineering, Sungkyunkwan University, Suwon 440-746, South Korea

Corresponding author: Keum Cheol Hwang (khwang@skku.edu)

This work was supported by the Institute of Information and Communications Technology Planning and Evaluation (IITP) Grant by the Korean Government through the Ministry of Science and Information and Communication Technologies (MSIT) (Development of low power/low delay/self-power suppliable RF simultaneous information and power transfer system and stretchable electronic epineurium for wireless nerve bypass implementation) under Grant 2020-0-00261.

ABSTRACT This paper presents a low-profile magneto-electric (ME) dipole antenna with an enhanced impedance bandwidth realized by the loading of shorting parasitic elements. The antenna contains a horizontal planar electric dipole antenna, a Γ-shaped shorted patch antenna, a pair of parasitic L-shaped shorted patches, and a direct feed. By loading of the parasitic L-shaped patches such that they are shorted to the ground, the proposed antenna attains a significant bandwidth enhancement while maintaining excellent broadside radiation characteristics. An antenna prototype with a low profile of only $0.11\lambda_0$ was fabricated and tested (λ_0 is the free-space wavelength referring to the center frequency). The antenna achieves a measured impedance bandwidth of 75.64% (1.34–2.97 GHz) for a voltage standing wave ratio (VSWR) of less than 2. Within the operating band, the measured gain ranges from 6.23 to 8.49 dBi. Additionally, stable radiation patterns on both E- and H-planes with a high front-to-back ratio of more than 20.5 dB are achieved.

INDEX TERMS Bandwidth enhancement, low profile, magneto-electric (ME) dipole, shorting parasitic element, wideband.

I. INTRODUCTION

A magneto-electric (ME) dipole antenna is a type of complementary antenna that consists of an electric dipole (formed by a horizontal planar half-wave dipole) and a magnetic dipole (formed by a vertical shorted quarter-wave patch) placed orthogonally. It is common knowledge that the electric dipole antenna has a radiation pattern in the shape of a Figure-8 on the E-plane and in the shape of a Figure-O on the H-plane, whereas, the magnetic dipole has a Figure-O radiation pattern on the E-plane and a Figure-8 radiation pattern on the H-plane [1], [2]. Therefore, when these two sources with equal amplitudes and phases are combined and simultaneously excited, the resultant ME dipole antenna exhibits identical and symmetrical radiation patterns on both the E- and H-planes. Moreover, as the electric dipole mode and magnetic dipole mode operate in adjacent frequency ranges, the ME dipole antenna achieves a wide impedance bandwidth, a stable and high gain, low back radiation, and low cross-polarization across the entire operating band [2], [3]. Given these excellent features, the ME dipole antenna has been widely studied and applied in modern wireless communication systems, especially in wireless base stations [4]–[7]. The conventional ME dipole antenna as initially presented in [8], however, is associated with the disadvantage of its relatively high profile of around $0.25\lambda_0$ (λ_0 is the free-space wavelength at the center frequency), resulting in inconvenience in some practical applications. Therefore, designing a wideband ME dipole antenna with a low profile has become a major concern in recent years.

To reduce the height of the ME dipole antenna, several techniques have been proposed [9]–[17]. By folding vertical shorted quarter-wave patches into different shapes along the z-axis [9], [10], the heights of the ME dipole antennas

The associate editor coordinating the review of this manuscript and approving it for publication was Hassan Tariq Chattha.

were decreased to $0.173\lambda_0$ and $0.169\lambda_0$, while the impedance bandwidths (IBWs) in cases for which VSWR < 1.5 for these antennas were 54.8% and 53.6%, respectively. A metamaterial loading technique was also introduced [11], helping to reduce the volume of the ME dipole antenna effectively without any degradation of the antenna performance, but its height was still $0.196\lambda_0$ and its IBW for VSWR < 2 was 44.1%. An ME dipole antenna with a height of $0.15\lambda_0$ was realized by loading with a high-permittivity dielectric substrate instead of an air substrate between two vertical shorted quarter-wave patches [12], achieving an IBW of 48.7%. In other work [13], by introducing an obtuse-triangular structure to act as a magnetic dipole, the height of the ME dipole antenna was reduced dramatically to $0.097\lambda_0$; however, the achievable IBW of this antenna was also reduced to 28.2%. Several low-profile substrate-integrated ME dipole antennas were also investigated [14], [15]. In those studies, the corresponding heights of these antennas were reduced to $0.11\lambda_0$ and $0.082\lambda_0$. However, these antennas achieved the IBWs of less than 20%. Recently, an ME dipole antenna with a low profile of $0.116\lambda_0$ that utilizes a pair of Γ-shaped shorted patches was presented, reportedly showing an IBW of 43.6% [16]. In another study [17], a defected ground structure was applied to an ME dipole antenna in order to enhance its IBW to 86.9%, but its height was increased to $0.23\lambda_0$. Clearly, it is very challenging to design an ME dipole antenna that can achieve a low-profile structure and a broad IBW simultaneously.

In this paper, a low-profile and broadband ME dipole antenna loading with shorting parasitic elements is proposed to address the above-mentioned problem. Based on the original design as available in the literature [16], a pair of parasitic L-shaped shorted patches is introduced to broaden the IBW significantly. The features of the proposed antenna are initially investigated using the ANSYS HFSS full-wave simulator and are validated experimentally through a fabricated prototype. Reasonable agreement is observed between the simulated and measured results. The measured IBW is 75.64% from 1.34 to 2.97 GHz with a maximum realized gain of 8.49 dBi at 2.75 GHz. Compared to an earlier design [16], the IBW of the proposed antenna is increased by a factor of 1.7 from 43.6 to 75.64% while maintaining an antenna profile of approximately $0.11\lambda_0$, hence achieving a wideband and low-profile design. In addition, the antenna exhibits stable radiation patterns, high FBRs, and low-cross polarization levels across the entire operating bandwidth.

The organization of this paper is as follows. Section II presents the antenna configuration, design procedure, operating principle, and the parametric studies. In Section III, the experimental results of the fabricated prototype are summarized and described, followed by the conclusion in Section V.

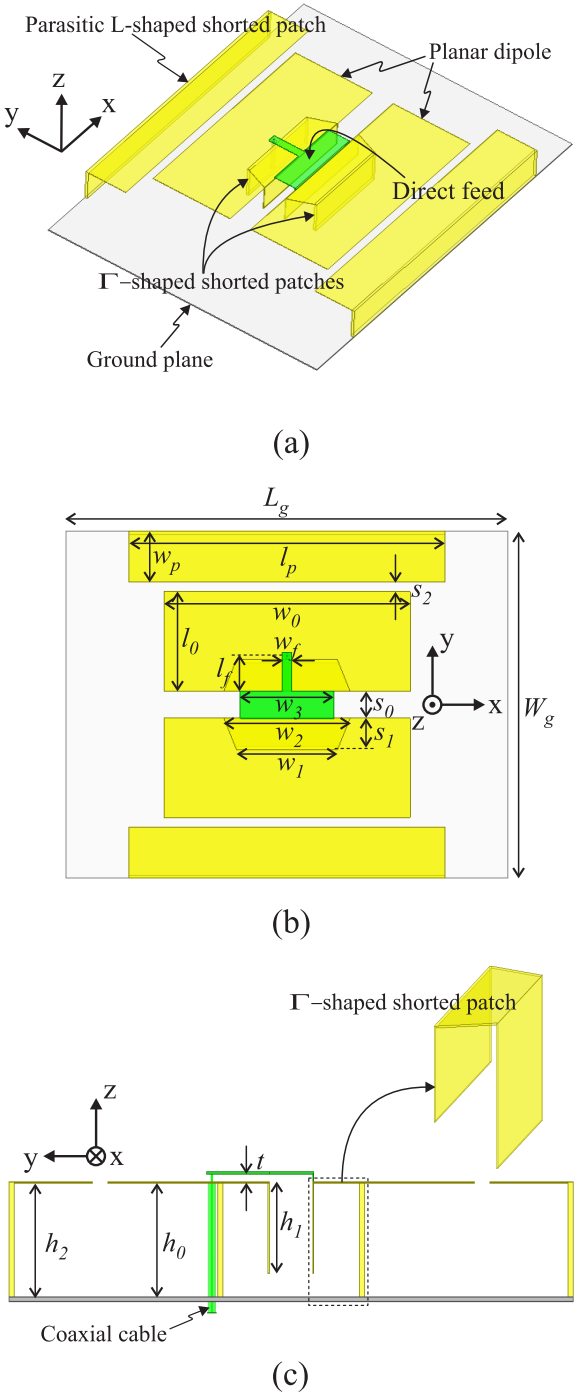

FIGURE 1. Configuration of the proposed low-profile wideband ME dipole antenna. (a) Three-dimensional view. (b) Plan view. (c) Side view.

II. ANTENNA DESIGN

A. ANTENNA CONFIGURATION

Figure 1 shows the configuration of the proposed ME dipole antenna with detailed dimensions. All dimensions of the proposed antenna, as optimized in a simulation, are listed in Table 1. The antenna consists of a pair of horizontal planar patches, a pair of Γ-shaped shorted patches, a pair of parasitic L-shaped shorted patches, a direct feed, and a rectangular ground plane. As shown in Figure 1, the two horizontal planar patches together operate as an electric dipole, whereas the open end at the center between the two vertical patches

TABLE 1. Dimensions of the proposed ME dipole antenna.

Parameter	W_g	L_g	w_0	l_0	w_p
Value/mm	110	140	78	31.5	16.25
	$0.79\lambda_0$	$1.0\lambda_0$	$0.56\lambda_0$	$0.23\lambda_0$	$0.12\lambda_0$
Parameter	l_p	w_1	w_2	w_3	w_f
Value/mm	100	32	40	29.5	3
	$0.72\lambda_0$	$0.22\lambda_0$	$0.29\lambda_0$	$0.21\lambda_0$	$0.022\lambda_0$
Parameter	l_f	s_0	s_1	s_2	h_0
Value/mm	12.2	8.5	9.2	3	14
	$0.088\lambda_0$	$0.061\lambda_0$	$0.066\lambda_0$	$0.022\lambda_0$	$0.1\lambda_0$
Parameter	h_1	h_2	t		
Value/mm	11.7	14	1		
	$0.084\lambda_0$	$0.1\lambda_0$	$0.007\lambda_0$		

λ_0 is the free space wavelength at the center frequency of 2.155 GHz.

operates as a magnetic dipole. The vertical patch is folded into a Γ-shaped form, which effectively reduces the overall height of the ME dipole [16]. The two parasitic L-shaped shorted patches are symmetrically located on two sides of the ME dipole antenna at a distance of s_2 from the horizontal planar patches. Each parasitic L-shaped shorted patch consists of one vertical rectangular plate and one horizontal rectangular plate. To excite the antenna, a direct feed is employed. The feed consists of a segment of 50-Ω coaxial cable and an air microstrip line. The coaxial cable goes through the ground plane and extends to one horizontal planar dipole. The outer conductor of the coaxial cable is connected to both the ground plane and one horizontal planar dipole. Meanwhile, the inner conductor of the coaxial cable is elongated along the $+z$-direction and is connected to one end of the horizontal air microstrip line at a distance of t from the horizontal planar dipole. The air microstrip line extends along one arm of the planar dipole, across the center gap, and then folds to connect to the other dipole arm directly. This feeding structure makes the antenna direct current (dc) grounded, which satisfies the requirement in some practical applications, such as the design of antennas for outdoor environment. The width of the feed line portion at the center is widened for better impedance matching.

B. OPERATING PRINCIPLE

The effect of the parasitic L-shaped shorted patches on the antenna performance is investigated. Figure 2 shows a comparison of the simulated VSWRs and input impedances of an antenna with parasitic L-shaped shorted patches (proposed antenna) and an antenna without parasitic L-shaped shorted patches (reference antenna). As shown in Figure 2(a), the reference antenna has an IBW (for VSWR < 2) of only 39.14% (1.87–2.78 GHz). Meanwhile, upon loading with parasitic L-shaped shorted patches, the impedance matching of the proposed antenna is significantly broadened, resulting in a broad IBW of 76.15% (1.35–3.01 GHz). An increase of approximately 1.9 times in the IBW is achieved by simply loading the parasitic L-shaped shorted patches. In addition, the starting operating frequency is significantly reduced from

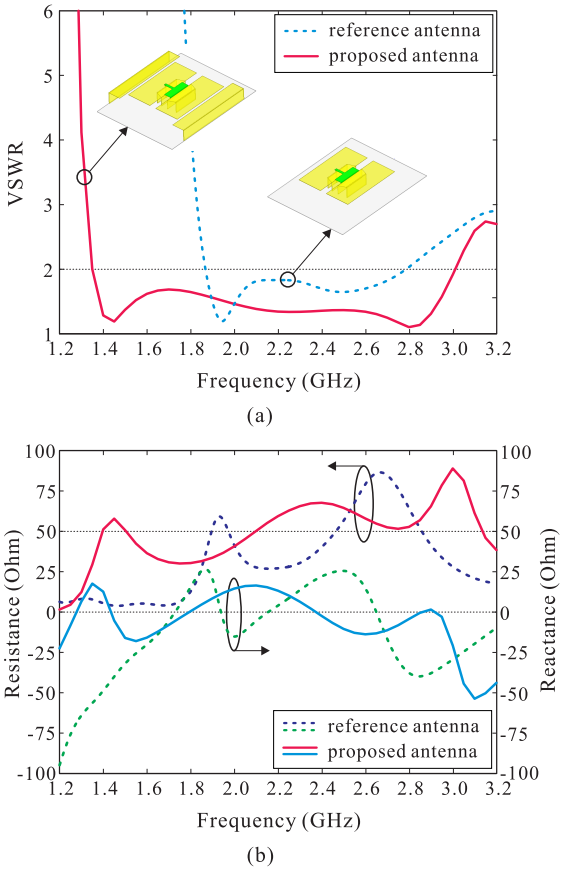

FIGURE 2. Effect of parasitic L-shaped shorted patches on the antenna performance. (a) VSWRs. (b) Input impedances.

1.87 GHz in the reference antenna to 1.35 GHz in the proposed antenna, indicating that a significant size reduction can also be achieved. To illustrate the inner resonance characteristics more clearly, Figure 2(b) presents the simulated input impedances of the two antennas. It can be observed that the parasitic L-shaped shorted patches contribute to attaining resonance in the lower frequency range. This additional structure introduces an equivalent inductive reactance load, which counteracts the large capacitive reactance in the reference antenna at frequencies below its operating band. Moreover, the input resistance of the proposed antenna at low band increases to nearly 50-Ω. As a result, the proposed antenna achieves good impedance matching over a wider frequency range.

To clearly explain how the lowest resonance at 1.4 GHz is generated, we studied the E-field distribution of the proposed antenna. The simulated E-field distribution at 1.4 GHz in the y-z cutting plane is shown in Figure 3. As observed, the E-field densities are mainly concentrated on two gaps between the horizontal planar dipole and the parasitic L-shaped shorted patches, thereby, the radiation at the lowest resonant frequency of 1.4 GHz is mainly from these two gaps. In addition, the E-field vectors on two gaps are in the same direction, hence producing the broadside radiation.

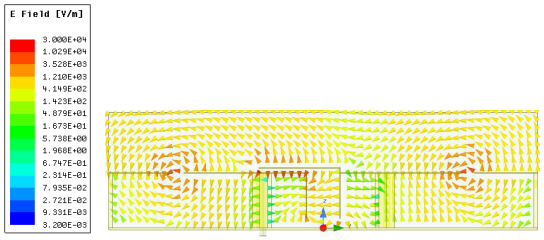

FIGURE 3. Simulated E-field distribution in the y-z cutting plane at 1.4 GHz.

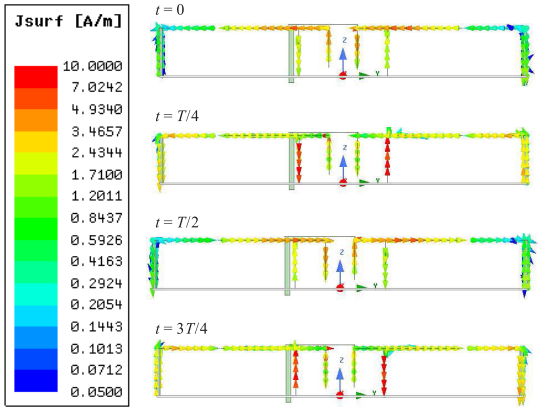

FIGURE 4. Current distributions of the proposed ME dipole antenna at different times.

As shown in Figure 4, the time-varying current distributions at 2.2 GHz are investigated to explain the working principle of the proposed ME dipole antenna. At time $t = 0$, the horizontal currents on two horizontal planar dipole arms dominate and are in one direction, while the vertical currents on two Γ-shaped shorted patches are minimized. Accordingly, the *y*-directional electric dipole mode is mainly excited at $t = 0$. At time $t = T/4$, where T is a period of time, the horizontal currents on two horizontal planar dipole arms become weak, while the vertical currents on two Γ-shaped shorted patches become strong and are in opposite directions. Therefore, the *x*-directional magnetic dipole mode is strongly excited at $t = T/4$. At time $t = T/2$, the electric dipole mode is mainly excited again with the current direction is opposite to that of the mode at $t = 0$. At time $t = 3T/4$, the magnetic dipole mode is strongly excited again with the current direction opposite to that of the mode at $t = T/4$. Therefore, it can be concluded that a typical ME dipole antenna is established.

C. PARAMETRIC STUDIES

To understand how the parasitic L-shaped shorted patch affects the performance of the antenna, a parametric study was conducted. Three parameters are selected for the parametric study: the gap s_2 between the parasitic L-shaped shorted patch and the horizontal planar dipole, the length of the parasitic L-shaped shorted patch l_p, and the height of the parasitic L-shaped shorted patch h_2. As one parameter

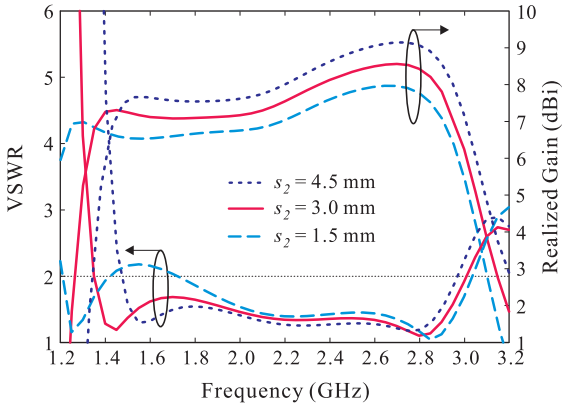

FIGURE 5. Simulated VSWRs and gains versus the frequency with different s_2 values.

is investigated, the others are assigned with the optimized values reported in Table 1.

Figure 5 shows the effect of the gap s_2 on the VSWR and the gain performance. Figure 4 shows the effect of the gap s2 on the VSWR and the gain performance. As observed from this figure, the gap s_2 determines both the frequency of the first resonance and the antenna gain. When s_2 decreases, the first resonant point moves toward a lower frequency and the antenna gain is also reduced. However, the VSWR at frequency of approximately 1.6 GHz exceeds 2 and the IBW splits when s_2 is decreased to less than 1.5 mm. Thus, $s_2 =$ 3.0 mm is finally selected for a wider IBW and better in-band matching.

Figure 6 demonstrates the effect of the width w_p on the VSWR and the gain performance. It is found that as w_p increases, the IBW reduces and slightly moves to lower frequency range. The starting operating frequency also slightly shifts to a lower frequency and the gain at high frequencies decreases when increasing w_p. Therefore, considering the tradeoff of the wide IBW and reduction of the starting operating frequency, the value of w_p is finally chosen as 16.25 mm.

Figure 7 depicts the VSWR and gain with different values of l_p. When increasing l_p, the IBW is slightly extended to a

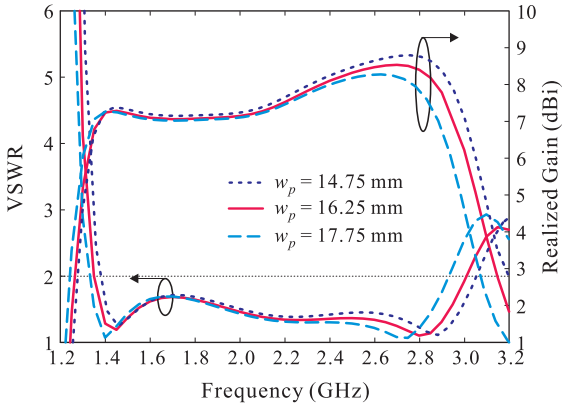

FIGURE 6. Simulated VSWRs and gains versus the frequency with different w_p values.

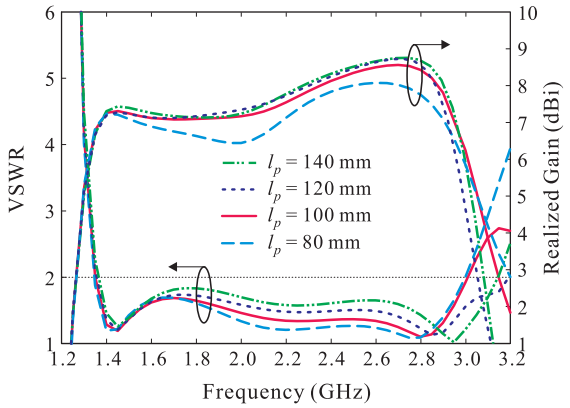

FIGURE 7. Simulated VSWRs and gains versus the frequency with different l_p values.

higher frequency and the gain in the middle frequencies is slightly increased. However, at frequencies above 3.0 GHz, the gain drops dramatically as l_p is increased to more than 100 mm. This occurs because these frequencies are more than twice the first resonance frequency, meaning that the higher order mode becomes the dominant mode, resulting in an increase of the cross-polarization level. Considering the wide IBW and good gain within the entire operating band, the optimal value of l_p is set to 100 mm.

The variations of the VSWR and gain with different values of h_2 are illustrated in Figure 8. It is found that as h_2 increases, the first resonance shifts to a lower frequency and the gain decreases slightly. Meanwhile, there is little effect on the second and third resonances. To achieve the widest IBW, the value of h_2 is finally optimized to 14 mm, which is also equal to the height h_0 of the proposed ME dipole antenna, hence maintaining the low profile characteristic.

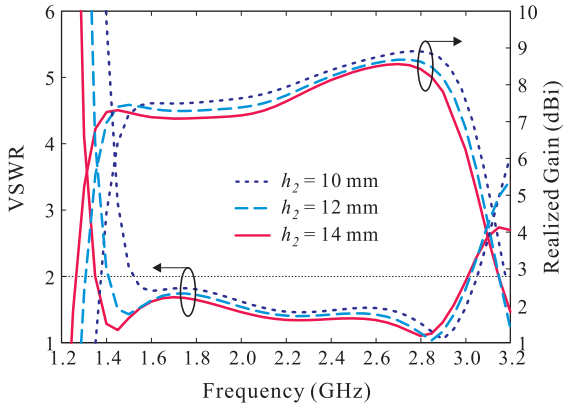

FIGURE 8. Simulated VSWRs and gains versus the frequency with different h_2 values.

III. EXPERIMENTAL RESULTS AND DISCUSSION

Based on the optimized design parameters listed in Table 1, a prototype of the antenna was built to verify the proposed design. Figure 9 shows a photograph of the fabricated

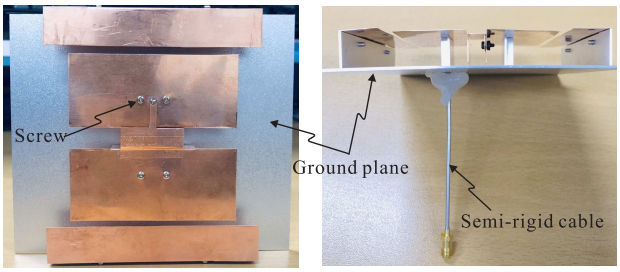

FIGURE 9. Photograph of the fabricated antenna.

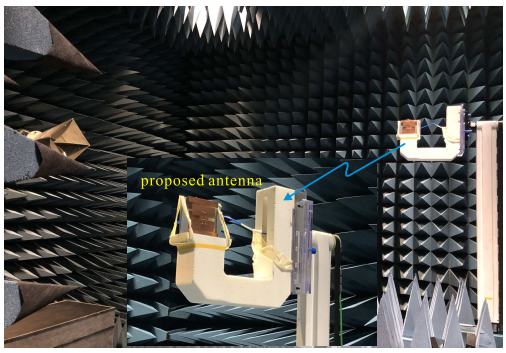

FIGURE 10. Measurement setup in an anechoic chamber.

antenna. The ground plane and vertical walls are made of aluminum with a thickness of 1 mm, while all other parts except the connector are made of copper with a thickness of 0.2 mm. Antenna components are combined using metal screws to assemble the final structure. A semi-rigid cable is used to realize the coaxial cable modeled in the simulation. The fabricated antenna is $110 \times 140 \times 15.2$ mm^3 in size, corresponding to $0.79 \times 1.0 \times 0.11\ \lambda_0{}^3$. In the measurement, the VSWR is determined by an Agilent 8510C vector network analyzer, and the antenna gain and radiation patterns are measured in a microwave anechoic chamber, as shown in Figure 10.

Figure 11 shows a comparison between the simulated and measured VSWRs. The measured IBW for VSWR < 2 is

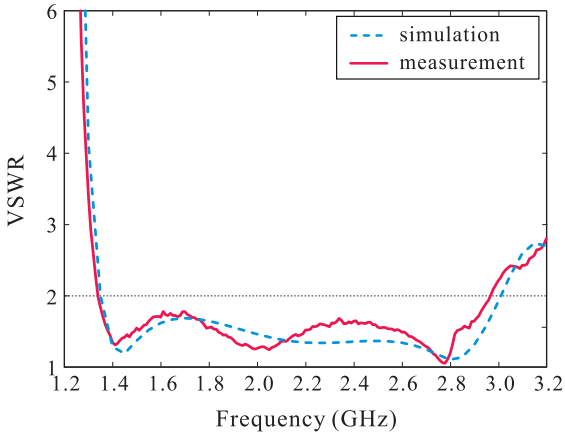

FIGURE 11. Measured and simulated VSWRs versus the frequency of the proposed ME dipole antenna.

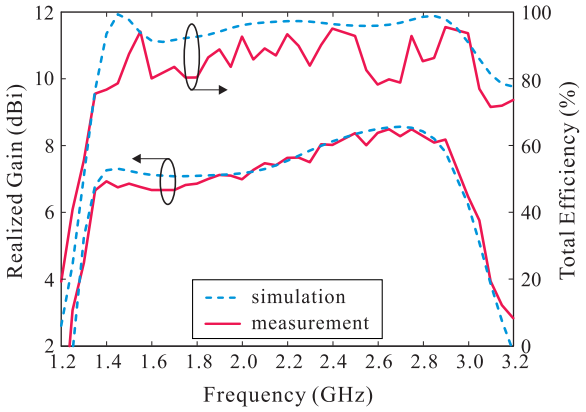

FIGURE 12. Measured and simulated gains and total efficiencies versus the frequency of the proposed ME dipole antenna.

TABLE 2. Measured 3-dB Beamwidth and front-to-back ratio (FBR).

3-dB Beamwidth			FBR (dB)
Frequency	E-plane	H-plane	
1.4 GHz	80°	87°	24.4
2.2 GHz	75°	87°	23.2
2.8 GHz	54°	53°	20.5

TABLE 3. Comparison between the proposed low-profile wideband ME dipole antenna and existing designs.

Ref.	Bandwidth [%]	Profile [λ_0/λ_L]	Peak Gain [dBi]	FBR [dB])
[11]	44.1	0.196/0.152	8.5	> 15.3
[12]	48.7	0.15/0.113	8.6	> 12.9
[13]	28.2	0.097/0.086	10.3	> 13
[16]	43.6	0.116/0.091	9.6	> 13
[17]	86.9	0.23/0.13	8.4	> 10
[18]	52.7	0.084/0.062	8	> 15.6
[19]	36	0.1/0.082	9.6	> 20
[20]	24.5	0.06/0.053	7.8	> 11
[21]	55	0.06/0.043	7	> 10
This work	**75.64**	**0.11/0.068**	**8.49**	**> 20.5**

λ_0 is the wavelength at the center frequency of the IBW in free space.
λ_L is the wavelength at the lowest frequency of the IBW in free space.

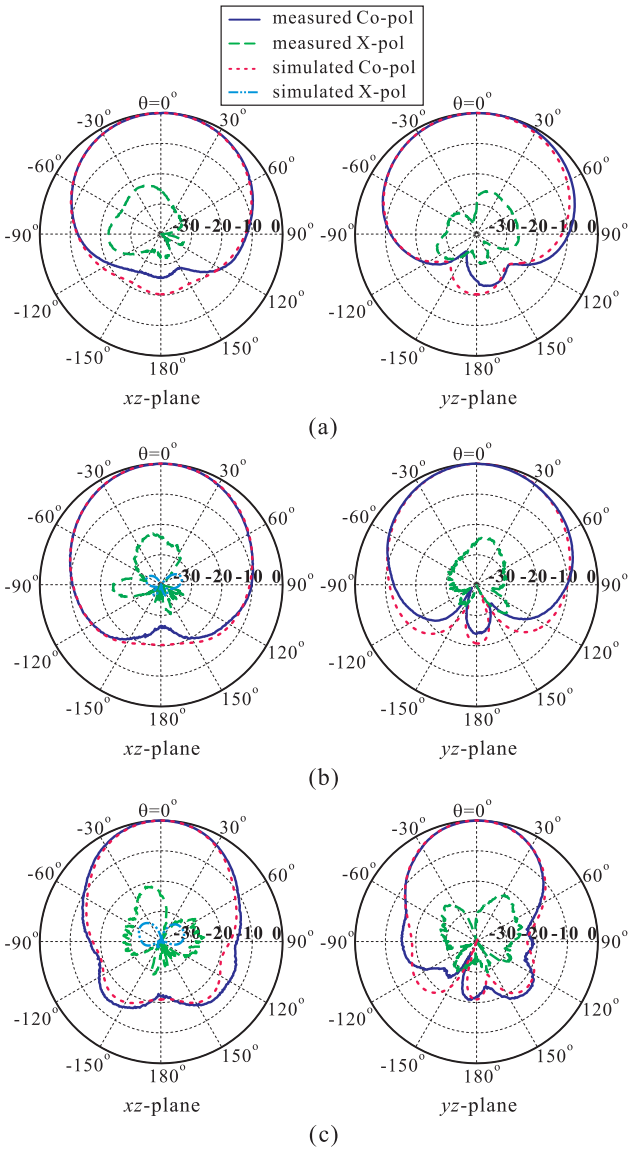

FIGURE 13. Simulated and measured normalized radiation patterns of the proposed ME dipole antenna at (a) 1.4 GHz, (b) 2.2 GHz, and (c) 2.8 GHz.

75.64% from 1.34 to 2.97 GHz. The simulated and measured gains and total efficiencies are given in Figure 12. As observed from this figure, the measured gain of the antenna exceeds 6.23 dBi across the entire operating frequency band with a maximum measured gain of 8.49 dBi at 2.75 GHz. The corresponding simulated gain is from 6.48 to 8.56 dBi. Figure 12 also shows a comparison between the simulated and measured total efficiencies. The average measured efficiency of the antenna is approximately 85.7% in the bandwidth from 1.34 to 2.97 GHz.

Figure 13 plots the simulated and measured normalized radiation patterns at 1.4, 2.2, and 2.9 GHz. Reasonable agreement was noted between the simulated and measured results, with some discrepancies mainly caused by fabrication imperfections and experimental tolerances. The antenna exhibits good unidirectional radiation patterns. Almost equal radiation patterns on the *xz*-plane (H-plane) and *yz*-plane (E-plane) are achieved across the operating frequency band. The measured cross-polarization level is below -21 dB over operational frequency range. It should also be noted that the simulated cross-polarization levels on the E-plane are less than -40 dB, which cannot be illustrated in the graphs. Table 2 summarizes the measured 3-dB beamwidth and front-to-back ratio (FBR). As observed, the 3-dB beamwidth becomes narrower when the frequency moves higher. The measured FBR is more than 23 dB at lower frequencies and drops slightly to 20.5 dB at 2.8 GHz.

A comprehensive comparison of the proposed low-profile wideband ME antenna and typical examples in the literature is carried out, with the results presented in Table 3. Compared to previous ME dipole antennas [11]–[13], [16], the proposed

antenna exhibits a much wider IBW and a higher FBR while maintaining a very low profile of only $0.11\lambda_0/0.068\lambda_L$. Although one earlier design [17] has a wider IBW, its height is nearly twice that of the proposed antenna. Compared to the other low-profile wideband antennas, such as a slot-loaded patch antenna [18], a slot-fed dipole-patch antenna [19], a hybrid metasurface antenna [20], and a differentially-fed patch antenna [21], the proposed antenna has the advantages of wider IBW and higher FBR. In addition, the proposed antenna also yields an acceptable gain for a common low-profile wideband antenna.

IV. CONCLUSION

A bandwidth-enhanced low-profile ME dipole antenna was presented in this paper. The proposed ME dipole antenna can be considered as an upgraded design of an earlier antenna [16] incorporated with a pair of parasitic L-shaped shorted patches to broaden the operating bandwidth significantly. In order to verify the performance of the antenna, a prototype was designed, fabricated, and examined. The experimental results demonstrated an impedance bandwidth of 75.64% from 1.34 to 2.97 GHz, a realized gain ranging from 6.23 to 8.49 dBi, a front-to-back ratio exceeding 20.5 dB, and stable radiation patterns. Moreover, the antenna has a low profile of only $0.11\lambda_0$. With these advantages and inherently dc grounded property, the proposed wideband low-profile ME dipole antenna is suitable to be used in outdoor environment.

REFERENCES

[1] C. A. Balanis, *Antenna Theory: Analysis and Deign*, 3rd ed. New York, NY, USA: Wiley, 2005.
[2] A. Chlavin, "A new antenna feed having equal E-and H-plane patterns," *Trans. IRE Prof. Group Antennas Propag.*, vol. 2, no. 3, pp. 113–119, Jul. 1954.
[3] A. Clavin, D. Huebner, and F. Kilburg, "An improved element for use in array antennas," *IEEE Trans. Antennas Propag.*, vol. AP-22, no. 4, pp. 521–526, Jul. 1974.
[4] K. M. Luk and B. Wu, "The magnetoelectric dipole—A wideband antenna for base stations in mobile communications," *Proc. IEEE.*, vol. 100, no. 7, pp. 2297–2307, Apr. 2013.
[5] L. Chang, J.-Q. Zhang, L.-L. Chen, and B.-M. Li, "Bandwidth-enhanced cavity-backed magneto-electric dipole antenna," *IEEE Access*, vol. 6, pp. 62482–62489, 2018.
[6] P. Mohammadi, M. Rezvani, and T. Siahy, "A circularly polarized wideband magneto-electric dipole antenna with simple structure for BTS applications," *AEU-Int. J. Electron. Commun.*, vol. 105, pp. 92–97, Jun. 2019.
[7] B. Feng, K. L. Chung, J. Lai, and Q. Zeng, "A conformal magneto-electric dipole antenna with wide H-plane and band-notch radiation characteristics for sub-6 GHz 5G base-station," *IEEE Access*, vol. 7, pp. 17469–17479, 2019.
[8] K.-M. Luk and H. Wong, "A new wideband unidirectional antenna element," *Int. J. Microw. Opt. Technol.*, vol. 1, no. 1, pp. 35–44, Jun. 2006.
[9] L. Ge and K. M. Luk, "A low-profile magneto-electric dipole antenna," *IEEE Trans. Antennas Propag.*, vol. 60, no. 4, pp. 1684–1689, Apr. 2012.
[10] L. Ge and K. M. Luk, "A magneto-electric dipole antenna with low-profile and simple structure" *IEEE IEEE Antennas Wireless Propag. Lett.*, vol. 12, pp. 140–142, 2013.
[11] M. Li, K.-M. Luk, L. Ge, and K. Zhang, "Miniaturization of magnetoelectric dipole antenna by using metamaterial loading," *IEEE Trans. Antennas Propag.*, vol. 64, no. 11, pp. 4914–4918, Nov. 2016.
[12] L. Siu, H. Wong, and K.-M. Luk, "A dual-polarized magneto-electric dipole with dielectric loading," *IEEE Trans. Antennas Propag.*, vol. 57, no. 3, pp. 616–623, Mar. 2009.
[13] C. Ding and K.-M. Luk, "Low-profile magneto-electric dipole antenna," *IEEE Antennas Wireless Propag. Lett.*, vol. 15, pp. 1642–1644, 2016.
[14] H. W. Lai and H. Wong, "Substrate integrated magneto-electric dipole antenna for 5G Wi-Fi," *IEEE Trans. Antennas Propag.*, vol. 63, no. 2, pp. 870–874, Feb. 2015.
[15] C. Shuai and G. Wang, "Substrate-integrated low-profile unidirectional antenna," *IET Microw., Antennas Propag.*, vol. 12, no. 2, pp. 185–189, Feb. 2018.
[16] L. Ge, S. Gao, D. Zhang, and M. Li, "Magnetoelectric dipole antenna with low profile," *IEEE Antennas Wireless Propag. Lett.*, vol. 17, no. 10, pp. 1760–1763, Oct. 2018.
[17] J. Zeng and K.-M. Luk, "A simple wideband magnetoelectric dipole antenna with a defected ground structure," *IEEE Antennas Wireless Propag. Lett.*, vol. 17, no. 8, pp. 1497–1500, Aug. 2018.
[18] W. An, X. Wang, H. Fu, J. Ma, X. Huang, and B. Feng, "Low-profile wideband slot-loaded patch antenna with multiresonant modes," *IEEE Antennas Wireless Propag. Lett.*, vol. 17, no. 7, pp. 1309–1313, Jul. 2018.
[19] M. Wang, Q. Zhu, and C. H. Chan, "Wideband, low-profile slot-fed dipole-patch antenna and array," *IEEE Antennas Wireless Propag. Lett.*, vol. 19, no. 12, pp. 2250–2254, Dec. 2020.
[20] E. I. Wei Liu, Z. N. Chen, X. Qing, J. Shi, and F. H. Lin, "Miniaturized wideband metasurface antennas," *IEEE Trans. Antennas Propag.*, vol. 65, no. 12, pp. 7345–7349, Dec. 2017.
[21] N. Liu, L. Zhu, W. Choi, and J. Zhang, "A low-profile differentially fed microstrip patch antenna with broad impedance bandwidth under triple-mode resonance," *IEEE Antennas Wireless Propag. Lett.*, vol. 17, no. 8, pp. 1478–1482, Aug. 2018.

SON TRINH-VAN was born in Hanoi, Vietnam, in 1986. He received the B.Sc.(Eng.) degree in electronics and telecommunications from the Hanoi University of Science and Technology, Hanoi, in 2010, and the Ph.D. degree from the Division of Electronics and Electrical Engineering, Dongguk University, Seoul, South Korea, in 2015. He is currently a Research Professor with the Department of Electrical and Computer Engineering, Sungkyunkwan University, Suwon, South Korea. His research interests include design of circularly polarized antennas and millimeter-wave antennas and arrays.

THAI VAN TRINH received the B.S. degree in electrical and electronics engineering from the Ho Chi Minh City University of Technology and Education (HCMUTE), Ho Chi Minh City, Vietnam, in 2017, and the M.S. degree in electrical engineering from the Seoul National University of Science and Technology, South Korea, in 2019. He is currently pursuing the Ph.D. degree with the Department of Electrical and Computer Engineering, Sungkyunkwan University, Suwon, South Korea. His research interests include antennas for ultra-high-definition television (UHD-TV), internal antennas, reconfigurable antennas, and EMI/EMC.

YOUNGOO YANG (Senior Member, IEEE) was born in Hamyang, South Korea, in 1969. He received the Ph.D. degree in electrical and electronic engineering from the Pohang University of Science and Technology (Postech), Pohang, South Korea, in 2002. From 2002 to 2005, he was with Skyworks Solutions Inc., Newbury Park, CA, USA, where he designed power amplifiers for various cellular handsets. Since March 2005, he has been with the School of Information and Communication Engineering, Sungkyunkwan University, Suwon, South Korea, where he is currently a Professor. His research interests include RF/mm-wave power amplifiers, RF transmitters, and DC-DC converters.

KANG-YOON LEE (Senior Member, IEEE) received the B.S., M.S., and Ph.D. degrees from the School of Electrical Engineering, Seoul National University, Seoul, South Korea, in 1996, 1998, and 2003, respectively. From 2003 to 2005, he was with GCT Semiconductor Inc., San Jose, CA, USA, where he was the Manager of the Analog Division and worked on the design of CMOS frequency synthesizer for CDMA/PCS/PDC and single-chip CMOS RF chip sets for W-CDMA, WLAN, and PHS. From 2005 to 2011, he was an Associate Professor with the Department of Electronics Engineering, Konkuk University. Since 2012, he has been with the School of Information and Communication Engineering, Sungkyunkwan University, where he is currently an Associate Professor. His research interests include implementation of power integrated circuits, CMOS RF transceivers, analog integrated circuits, and analog/digital mixed-mode VLSI system design.

KEUM CHEOL HWANG (Senior Member, IEEE) received the B.S. degree in electronics engineering from Pusan National University, Busan, South Korea, in 2001, and the M.S. and Ph.D. degrees in electrical and electronic engineering from the Korea Advanced Institute of Science and Technology (KAIST), Daejeon, South Korea, in 2003 and 2006, respectively.

From 2006 to 2008, he was with Samsung Thales, Yongin, South Korea, where he was involved in the development of various antennas for wireless communication and radar systems. From 2008 to 2014, he was an Associate Professor with the Division of Electronics and Electrical Engineering, Dongguk University, Seoul, South Korea. In 2015, he joined the Department of Electrical and Computer Engineering, Sungkyunkwan University, Suwon, South Korea, where he is currently a Professor. His research interests include advanced electromagnetic scattering and radiation theory and applications, design of multi-band/broadband array antennas, and optimization algorithms for electromagnetic applications.

Prof. Hwang is a Life Member of KIEES and a member of IEICE.